A polynomial regression model for predicting knuckleball movements in soccer free-kick

Jiahang Liu, Undergraduate student, *College of Mathematics, Jilin University, Changchun 130015, People's Republic of China;* Email: liujh1020@mails.jlu.edu.cn

Dongfang Liang, Professor, Department of Engineering, University of Cambridge, Cambridge, CB2 1PZ, United Kingdom; Visiting Professor, International Research Organization for Advanced Science and Technology, Kumamoto University, Kumamoto 860-8555, Japan; Email: dl359@cam.ac.uk

Hiroshi Cho, Professor, Faculty of Advanced Science and Technology (FAST), Kumamoto University, Kumamoto 860-8555, Japan; hcho@kumamoto-u.ac.jp

ABSTRACT

This paper develops a polynomial regression model with physical constraints to comprehensively analyze the complex motion of knuckleballs in soccer free-kick. The predictions match accurately with the ball trajectories extracted from recorded soccer matches. The model uses a polynomial function to account for the ball's projectile-like motion. It further incorporates a critical physical constraint that is related to the aerodynamic drag force on the ball. The regression model is implemented using a relaxed iterative method. The *lsqlin* solver of MATLAB is used in each iteration. The model is verified through a prominent case study – Cristiano Ronaldo's representative knuckleball free-kick executed in April 2012. The ball trajectory is meticulously derived from image processing of video footage. The paper examines the ball position, velocity and drag coefficient over the entire flight of the ball. Notably, a significant increase in the drag coefficient is observed during the flight, which is a critical feature of the knuckling effect. The study extensively explores the influence of physical constraints and various model parameters to ensure the regression model's credibility, shedding light on the intricate dynamics of knuckleball free-kicks. With its simplicity, efficiency and effectiveness, this polynomial regression model can be a powerful tool for studying knuckleball free-kicks in real time and thus improving players' techniques in training and in the match. Besides, it can be used to create authentic flight paths of the ball in computer games.

Keywords: Knuckleball free-kick; polynomial regression model; physical constraint; drag coefficient; soccer; football

Introduction

Free-kick are important goal scoring opportunities in soccer games, which require skillful control of the ball's motion to surpass both the defensive player wall and the goalkeeper. Some players opt for powerful strikes, attempting to blast the ball through the wall, while others choose to spin the ball, curling the ball over or around the wall.[1] Among these techniques, knuckleballs stand out as one of the most challenging, yet effective, shooting techniques, owing to the resulting unpredictable and erratic ball trajectories.[2] In this method, minimal spin is applied to the ball, making it difficult for opponents to predict its trajectory and defend against it.

The knuckleball technique first originated in baseball, popularized by the Major League Baseball pitcher E Cicotte in 1908.[3] Mastering this unique pitching skill earned Cicotte the nickname 'Knuckles', and he finished his career with over 200 wins.[4] In soccer, this technique has been adapted and employed by skillful players like Andrea Pirlo[5] and Cristiano Ronaldo[6] for executing long shots and free-kick. In soccer, the ball's flight often exhibits anomalous horizontal shaking or rapid falling, known as the 'knuckling effect'.[7] This effect often tricks goalkeepers' attempts to handle such shots effectively, making the knuckleball a formidable weapon in the game.

When a soccer ball travels through the air, it experiences both gravitational and aerodynamic forces. The latter force can be further separated into two components known as drag and lift. Lift represents the aerodynamic force component perpendicular to the ball's velocity and its magnitude is linked to the ball's spinning.[8] On the other hand, drag corresponds to the aerodynamic force component opposite to the ball's velocity, and its intensity is influenced by various factors, including the ball's flight speed, surface pattern,[9]

seam geometry[10] and air properties.[11] According to aerodynamics, the drag on a soccer ball is primarily caused by the pressure difference between its front and rear surfaces, due to the boundary layer separation. As the ball's speed increases to a critical value, a sudden drop in drag occurs due to a transition from laminar flow separation to turbulent separation. The phenomenon is referred to as the drag crisis, and the speed at which the drag coefficient reaches its minimum at the transition is termed the critical speed.[12] The critical speed is influenced by the surface roughness. It is believed that at this critical point the knuckling effect kicks in as a result of the asymmetric flow separation arising from the seams and other sources of asymmetry during the boundary layer separation.

Knuckleball has fascinated soccer players and viewers, especially after the 2006 World Cup when the design of the soccer ball changed greatly.[2] Mizota et al. employed wind tunnel experiments to study the motion characteristics of low-speed spinning soccer balls.[13] They attributed the knuckleball's motion characteristics to the wake and non-constant forces acting on the ball. Asai and Kamemoto, using two high-speed cameras and smoke flow visualization techniques, investigated the trajectories of knuckleball shots and determined the range of the Reynolds number associated with knuckleball motion.[14] The shedding of the wake vortices was also observed. Texier et al. summarized the knuckleball phenomenon in various sports and, through wind tunnel experiments, studied the swing period of the ball and established that the non-constant variation of wake vortices causes the swinging motion of knuckleballs.[15] Barber et al., employing computational fluid dynamics, examined the forces acting on knuckleballs and found that non-spinning soccer balls experience minimal lateral forces, causing their trajectories to be unpredictable with even slight disturbances.[16] They also compared the impact of different soccer ball brands on their motion characteristics.

These studies utilized wind tunnels, videos, CFD and other methods to investigate the aerodynamics and motion trajectories of knuckle soccer balls under specific conditions. However, research on knuckleball free-kicks in actual soccer matches remains scarce, although a vast amount of video data has been accumulated from numerous soccer matches.

Compared to well-designed experiments or simulations, the knuckleball free-kicks recorded in the soccer match contain large uncertainties. Hence, advanced data processing methods are necessary. In this study, we developed a polynomial regression model with physical constraints to comprehensively analyze the trajectory of the knuckleball free-kick in a real match, and then the aerodynamic process was investigated.

The remainder of this paper is structured as follows. The following section presents the data of a representative knuckleball free-kick executed by Cristiano Ronaldo. The next section derives a physical constraint after analyzing the aerodynamics of knuckleball free-kicks. The subsequent section presents a polynomial regression model with physical constraints and the numerical realization in MATLAB. Then, the results of the representative knuckleball are given and the influence of physical constraints and model parameters are analyzed. Finally, the concluding remarks are presented.

Acquisition and Processing of Video Data

A knuckleball free-kick goal scored by Cristiano Ronaldo in a match between Real Madrid and Atletico Madrid is regarded to be one of his best goals.[17] The 33rd round match of the 2011-2012 Spanish La Liga was held in Vicente Calderón Stadium, Madrid, Spain, and the free-kick goal occurred at about 9:30 pm, April 11, 2012. According to the weather data for Madrid, the air temperature was about 13 ℃, the air pressure was 705 mmHg, and the relative humidity was 54%.[18] Accordingly, the air density was 1.1401 kg/m^3 and the air kinetic viscosity was 1.560×10^{-5} m^2/s. The soccer ball used in the match was Nike Seitiro(Nike, Beaverton, USA), with a 0.7 m circumference and 0.44 kg weight.[19]

The video of this free-kick was downloaded from internet, which provides a large volume of information about this knuckleball free-kick. The video is 12 seconds in length with a frame rate of 30 frames per second. The video was split into individual frames using ACDSee (ACDSee 2020 Ultimate, ACD Systems International Inc, Victoria, Canada). A total of 39 images were selected. Using Photoshop software, these images were skillfully matched

together based on the distinctive features of players, soccer field and lawn stripes after the transparency was adjusted. Subsequently, the soccer field lines, including penalty area and goal area lines, were drawn for scaling the soccer ball trajectory later. The specific location of the soccer ball in each image was identified and marked. In this way, the trajectory of the free-kick was determined. By assuming the trajectory of the ball is on a vertical plane, the projection of the ball's flight trajectory on the ground, along with the height of the ball in each frame, were obtained, as shown in Fig. 1.

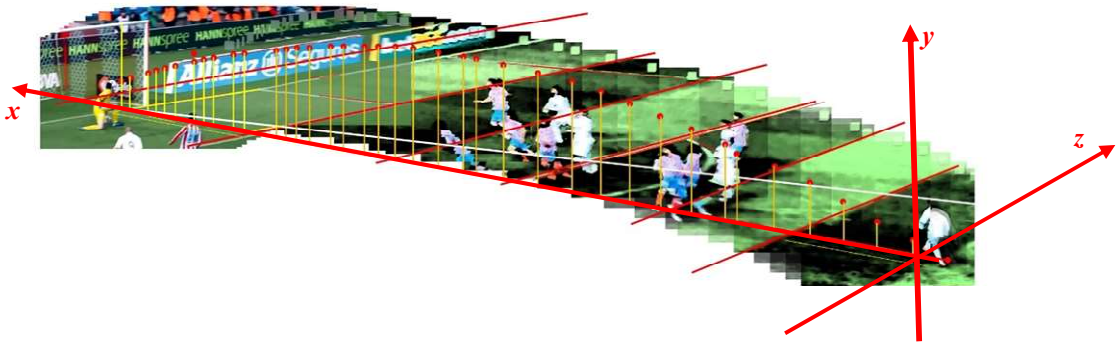
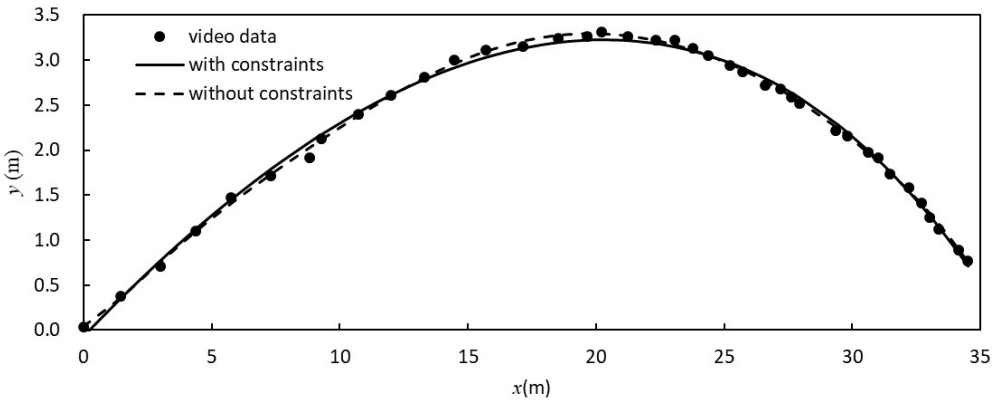


Fig. 1. Image matching of the video, with the ball's trajectory and projection on the ground.

According to the FIFA regulations, the penalty area is 40.32 m in width and 16.5 m in length, while the goal area is 18.32 m in width and 5.5 m in length. The goal stands are at a height of 2.44 m and have a width of 7.32 m. Integrating these dimensions, we established the horizontal and vertical scales for the trajectory curve in Fig. 1 and calculated the coordinates of the free-kick's trajectory, represented by the red dots in Fig. 2. The image resolution is around 6 mm/pixel. Assuming an error of ±1 pixel in aligning the soccer ball locations between images, we estimate that the dots involve ±6mm uncertainty. It can be observed that the free-kick was taken from approximately L = 35 m away from the gate, which is consistent with the information reported in the news.[17] The soccer ball reached its highest point at a distance of around x = 20 m, with a maximum height of approximately 3.3 m. Over the final 15 meters, the ball descended rapidly, making the trajectory different from a parabola.



127

128 **Fig. 2.** Trajectories of the studied knuckleball free-kick, where dots represent discrete points
129 obtained from the recorded video, the solid line represents fitting curve with physical
130 constraints, and the dashed line represents fitting curve without physical constraints.

131 **Aerodynamics of Knuckleball Flight**

132 This section derives a physical constraint related to the variation of the drag coefficient during
133 the ball's flight, based on the aerodynamic analysis of a knuckleball free-kick.

134 ***Force Analysis***

135 Due to the negligible spin of a knuckleball free-kick during its flight, lift from the Magnus
136 effect is ignored in this study. In the process of flight, it is impossible for a football to entirely
137 avoid rotation. However, in the study of Cristiano Ronaldo's free-kick, the impact of rotation
138 is negligible. Based on the video, Cristiano Ronaldo's free-kick had an airborne time of about
139 1.33 seconds, completing less than three rotations in the air, with a nearly uniform rotational
140 speed. The angular velocity thus remains consistently below 8π. Based on Kray et al.,[20] the
141 Magnus force coefficient (C_M) for the soccer ball remains below 0.1 and the magnitude of the
142 Magnus force exerted on the ball is below 0.5 N. In light of these calculations, the exclusion
143 of the Magnus force is justified.

144 Additionally, this study does not consider the swing motion due to the unsteady aerodynamic
145 force in the transverse direction. While it can significantly interfere with the goalkeeper's

judgment, the swing's impact on the overall flight trajectory is extremely subtle and often uncertain. A soccer ball with very slow rotation is more susceptible to the influence of natural wind during flight, resulting in a noticeable sway. Moreover, variations in the soccer ball's surface at the seams can also induce asymmetrical airflow and sway. Similarly, spin also alters the airflow and causes sway. Nevertheless, the sway in our studied case is insignificant. It is highly challenging to accurately extract the sway information from the video recordings available to us, so our study assumes the problem to be vertical two-dimensional.

Therefore, the knuckleball is mainly subjected to gravity and drag during its flight in the air (Fig. 3), and its trajectory is restrained on a vertical plane. Neglecting any deformation of the ball during flight, the two forces acting on the ball can be expressed as follows:

$$G = Mg \tag{1}$$

$$D = -\frac{1}{2}\rho C_D A V^2 \tag{2}$$

where G is the gravity force, M is the mass of soccer ball, g is the gravitational acceleration with a value of 9.81 m/s², D is the drag force, ρ is the air density, C_D is the drag coefficient, A is the frontal area of the soccer ball, and V is the soccer ball speed during the flight.

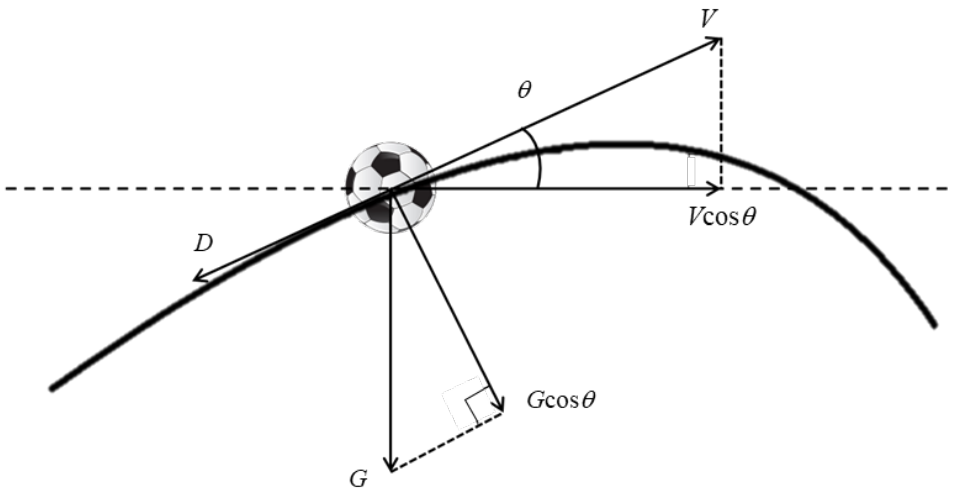


Fig. 3. Force analysis of a flying non-spin soccer ball in air, where G is the gravity force, D is the drag force, V is the flying speed, and θ the angle between flying direction and horizontal plane.

In a soccer game, the drag on the ball is dominated by pressure difference induced by boundary layer separation. The speed of the soccer ball mainly ranges between 5 m/s and 32 m/s in a match.[21] At a relatively low speed where the laminar boundary layer separation occurs, the drag coefficient keeps approximately constant. When the speed increases to a critical value where the boundary layer separation becomes turbulent, a remarkable reduction in the drag coefficient can be observed. Over the critical speed, the drag coefficient remains unchanged at a relatively low value. The change in the drag coefficient versus ball speed can be approximately expressed using a Sigmoid function based on Goff and Carre:[8]

$$C_D = a + \frac{b}{1 + \exp\left(\frac{V - V_c}{V_s}\right)} \tag{3}$$

where a = 0.155, b = 0.346, V_c = 12.19 m/s, and V_s = 1.309 m/s for Adidas Teamgeist soccer balls (Adidas, Herzogenaurach, Germany). These parameters can vary depending on surface patterns and air conditions. Tada et al.'s experiments[22] determined that a ranges from 0.15 to 0.3, and a + b ranges from 0.48 to 0.52. Specifically, for Nike Flight soccer balls (Nike, Beaverton, USA), tunnel aerodynamic experiments have shown that a = 0.24 and b = 0.30.[23-25] In this study, the values of a, b and V_s are taken from Goff et al., where they were calibrated through trial and error. The critical speed V_c represents the speed at which the transition from laminar boundary layer separation to turbulent separation occurs. The critical speed is not specific in a soccer match, because it is heavily related to the roughness of the soccer ball's surface and air conditions. In this context, the critical speed V_c is eliminated from Eq. 3, by introducing a relationship between the drag coefficient and its derivative. Differentiating the drag coefficient C_D with respect to speed V yields the following expression:

$$\frac{dC_D}{dV} = \frac{b}{V_s} \frac{\exp\left(\frac{V - V_C}{V_S}\right)}{\left[1 + \exp\left(\frac{V - V_C}{V_S}\right)\right]^2} \tag{4}$$

Eliminating the exponential function by combining Eqs. 3 and 4 results in an equation as:

$$\frac{dC_D}{dV} = -\frac{1}{V_s b}[C_D - a][C_D - (a+b)] \tag{5}$$

Dynamic Analysis

Subjected to the influence of gravity and drag, the soccer ball may alter its velocity, producing a trajectory depicted in Fig. 2. The ball's acceleration can be dissected into tangential and normal components. In the normal direction, only the gravity force is at play, affording some convenience to explore the relationship between the motion trajectory and velocity.

According to Newton's second law, the force acting on an object is equal to the product of the object's mass and its acceleration. In the normal direction of the soccer ball's motion, Newton's second law can be applied as follows:

$$G\cos\theta = ma_n \tag{6}$$

where θ represents the angle between the soccer ball's moving direction and the horizontal, and a_n represents the normal acceleration of the soccer ball. According to the dynamic principle in the intrinsic coordinates, the normal acceleration a_n can be formulated as follows:

$$a_n = \frac{V^2}{R} \tag{7}$$

where R is the curvature radius of the motion trajectory.

As shown in Fig. 1, a Cartesian coordinate system is established with the soccer ball's starting position as the origin, the horizontal and vertical as the x-axis and y-axis, respectively. Accordingly, the motion trajectory is represented as the function of $y = f(x)$. Given the projectile nature of the motion, the function $f(x)$ is expected be convex and its curvature radius R is formulated as:

$$R = -\frac{\left(1+f'^2\right)^{2/3}}{f''} \tag{8}$$

The angle between the soccer ball's moving direction and the horizontal plane is expressed as:

$$\cos\theta = \frac{1}{\left(1+f'^2\right)^{1/2}} \tag{9}$$

Substituting Eqs. 1, 7, 8, and 9 into Eq. 6, the soccer ball's speed V can be derived as:

$$V = \sqrt{-\frac{g\left(1+f'^2\right)}{f''}} \tag{10}$$

Then, the horizontal component of velocity is:

$$V_x = \sqrt{-\frac{g}{f''}} \tag{11}$$

During the soccer ball flight, the horizontal motion is exclusively influenced by the drag force. Therefore, applying Newton's second law in the horizontal direction yields the following expression:

$$D\cos\theta = ma_x \tag{12}$$

where a_x denotes the horizontal component of acceleration, which can be expressed as:

$$a_x = \frac{dV_x}{dt} = V_x\frac{dV_x}{dx} = \frac{1}{2}\frac{dV_x^2}{dx} = \frac{1}{2}g\frac{f'''}{f''^2} \tag{13}$$

Substituting Eqs. 2, 6, 10, and 13 into Eq. 12, the drag coefficient can be formulated as:

$$C_D = \frac{m}{\rho \mathrm{A}}\frac{f'''}{f''\sqrt{1+f'^2}} \tag{14}$$

Taking the derivative of Eq. 14 with respect to x yields the following expression:

$$\frac{dC_D}{dx} = \frac{m}{\rho A}\frac{1}{f''\sqrt{1+f'^2}}\left[f'''' - \left(\frac{f'''}{f''} + \frac{f'f''}{1+f'^2}\right)f'''\right] \tag{15}$$

By combining Eqs. 5 and 15, and utilizing Eq. 10, the following relationship is obtained:

$$f'''' - c_1 f''' = d_1 \tag{16}$$

where

$$c_1 = \frac{f'''}{f''} + \frac{f' f''}{1 + f'^2} \tag{17}$$

$$d_1 = \frac{\rho A \sqrt{g}}{2 m V_S b} [C_D - a][C_D - (a+b)] \sqrt{-f''} \left[\frac{\left(1 + f'^2\right) f'''}{f''} - 2 f' f'' \right] \tag{18}$$

Regression Model and Program Implementation

To quantitively analyze the trajectory and aerodynamics of knuckleball free-kicks, it is essential to reproduce the discrete points depicted in Fig. 2. The fitting process is combined with a physical constraint derived from the proceeding aerodynamic analysis. Given the projectile nature of the trajectory, a polynomial function is used to accurately fit the trajectory of the soccer ball's flight:

$$y = f(x;\alpha) = \sum_{i=0}^{n} \alpha_i \left(\frac{x}{L} \right)^i \tag{19}$$

where n is the order of the polynomial, $\alpha = [\alpha_0, \alpha_1, \cdots, \alpha_n]^T$ contains the independent parameters of the polynomial function, L = 35 is the horizontal distance of the soccer ball's flight. The reason for dividing x by L is to prevent the higher-order fitting coefficients from becoming too small. This formulation also allows for the expression of various orders of derivatives of the trajectory as polynomial functions. Through the application of the least squares method, the parameters α can be determined by minimizing the sum of the squared errors between the fitted curve and the discrete points. The least squares problem can be mathematically represented as:

$$\min_{\alpha} \sum_{j=1}^{m} \left[y_j - f(x_j;\alpha) \right]^2 \tag{20}$$

where x_j and y_j represent the horizontal and vertical coordinates of the discrete points in Fig. 2, m corresponds to the number of discrete points with a value of m = 39 in the present study.

To ensure that the trajectory fitting function accurately represents the aerodynamics of the flight object, it is important to incorporate appropriate physical constraints into the least

squares problem defined in Eq. 20, such as the relationship specified in Eq. 16. However, for the least squares problem outlined in Eq. 20 to have a unique solution, the inequality condition $m > n + 1$ must be met. Nevertheless, adhering to this inequality would render Eq. 16 impossible to hold for all discrete points. Accordingly, the equality constraint from Eq. 16 is reformulated into an alternate least squares problem as indicated below:[26]

$$\min_{\alpha} \sum_{j=1}^{m} \left[f''''(x_j;\alpha) - c_1(x_j;\alpha) f'''(x_j;\alpha) - d_1(x_j;\alpha) \right]^2 \tag{21}$$

Then, the least squares problem of Eq. 20 with the equality constraint of Eq. 16 is reconstructed as a double-objective least squares problem as follow:

$$\min_{\alpha} \sum_{j=1}^{m} \left\{ \left[y_j - f(x_j;\alpha) \right]^2 + \lambda \left(\frac{L}{2} \right)^8 \left[f''''(x_j;\alpha) - c_1(x_j;\alpha) f'''(x_j;\alpha) - d_1(x_j;\alpha) \right]^2 \right\} \tag{22}$$

where λ is an empirical weighting factor between the two least squares problems. A multiplier related to $L/2$ is included to normalize the second least squares problem, considering that Eq. 16 involves the fourth-order derivative of Eq. 12.

Directly solving the nonlinear least squares problem defined in Eq. 22 presents a challenge. To address this problem, a relaxed iterative algorithm, coupled with the available solver *lsqlin* in MATLAB, is used to resolve the proposed regression model for knuckleball free-kicks. The *lsqlin* solver is adept at tackling linear least squares problems,[27] making it well-suited for this specific model in each iteration. The procedure for the iterative computation is:

(1) Initialize model parameters such as a, b, V_s, λ, and n, and input the discrete data (x_j, y_j) of the knuckleball free-kick trajectory.

(2) Assign initial values to the polynomial parameter α in Eq. 19.

(3) Compute the coefficients c_1 and d_1 using Eqs. 17 and 18, based on the initially provided polynomial parameter α.

(4) Calculate the input parameters for the *lsqlin* solver, and subsequently update the polynomial parameter α through a relaxation method following the invocation of the *lsqlin* function.

(5) Iterate through steps (3)-(4) until convergence of the polynomial parameter α.

Results and Discussion

The analysis of moving trajectory and aerodynamics of the knuckleball free-kick is the focus of this section. Subsequently, an exploration of the impact exerted by the physical constraint and the specific model parameters is undertaken to underscore the regression model's versatility and sensitivity.

Motion Characteristics of Knuckleballs

Utilizing a polynomial order of n=9 and choosing a weight factor of $\lambda = 0.1$, the proposed regression model is solved using the discrete data, air conditions and soccer ball' measurements detailed in the proceeding sections. This process yields the value of polynomial parameter α = [-0.0724, 10.4640, -7.0799, -1.6177, -0.8602, 3.9957, -10.1578, 8.9066, -3.5557, 0.4920]^T.

Based on the acquired polynomial parameter, the trajectory of the knuckleball free-kick is plotted, as shown by the solid line in Fig. 2. The coefficient of determination[28] is calculated as R^2=0.9962, which is high, signifying a high precision of the fitting curve.

The soccer ball's flight speed is calculated using Eq. 10, and the ball's evolution along the trajectory is graphed, as depicted by the solid line in Fig. 4. The initial speed of the airborne soccer ball is estimated to be approximately 31 m/s (or 111.6 km/h), gradually decreasing until it reaches approximately 17 m/s at the gate. Although a specific speed for this particular knuckleball free-kick is not documented in any report, the calculated speed aligned well with attributes of a typical free-kick executed by Cristiano Ronaldo. It is recognized that Ronaldo is capable of striking a free-kick at speeds up to 105 km/h,[29] which roughly substantiates the present prediction.

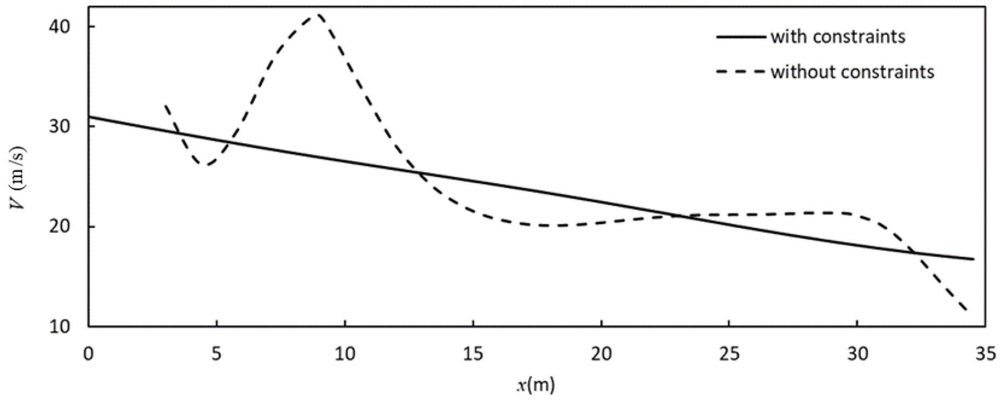


Fig. 4. Changes in flight speeds of knuckleball free-kick calculated with and without constraints.

The variation of the knuckleball drag coefficient CD along the trajectory was calculated using Eq. 14 and is depicted in Figure 5. The drag coefficient starts at a relatively low value and exhibits a gradual change, consistently remaining below C_D = 0.25. Beyond the distance of x=15m, there is a rapid surge in the drag coefficient, approaching C_D = 0.5 at around x=25m, after which it remains relatively steady. Applying Eq. 3, the transition from turbulent boundary layer separation to laminar separation is estimated to occur at around x = 19.5 m, corresponding to a critical speed of V_c = 22 m/s. This value slightly surpasses the one reported by Goff et al.;[8] however, it still falls within the range of soccer ball speeds associated with knuckleballs, as summarized by Texier et al.[15]

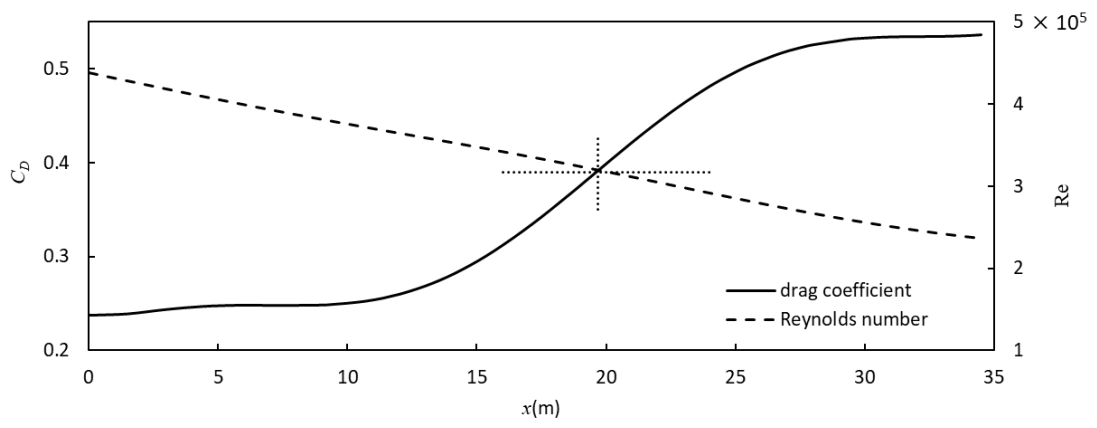


Fig. 5. Changes in drag coefficient and Reynolds number of the knuckleball free-kick calculated with physical constraints.

Fig. 5 also shows the variation of the Reynold number along the trajectory, where the Reynolds number is defined as $\mathrm{Re} = Vd/\nu$ with ν being the air kinetic viscosity and d being the soccer ball's diameter. As with the soccer ball's speed, the Reynold number exhibits a consistent decrease, starting at an initial value of 4.38×10^5 and reaching a terminal value of 2.36×10^5. The critical Reynold number at the transition point is around 3.18×10^5, approximately aligned with the established critical Reynolds number of 3.0×10^5 for a soccer ball.[30] Notably, the elevation of Madrid may facilitate Cristiano Ronaldo's ability to execute an excellent knuckleball due to a relatively small kinetic viscosity resulting from the low air pressure.

Fig. 6 shows the horizontal and vertical components of the ball's velocity. Initially, the vertical velocity is about 9 m/s, gradually diminishing to zero at the apex of the trajectory around x = 20 m. Subsequently, the ball descends, with an increasing absolute value. Deviating from the ideal projectile motion, the terminal vertical velocity magnitude is notably smaller than its initial value, influenced by the air drag. Considering the horizontal velocity, it also undergoes a consistent reduction. Nonetheless, the horizontal velocity experiences a more rapid decline in the range of x > 19.5 m, resulting in a pronounced descent trajectory. This distinctive trajectory is one of the factors that earned this type of free-kick the nickname "knuckleball", which adversely affects the goalkeeper's judgment.

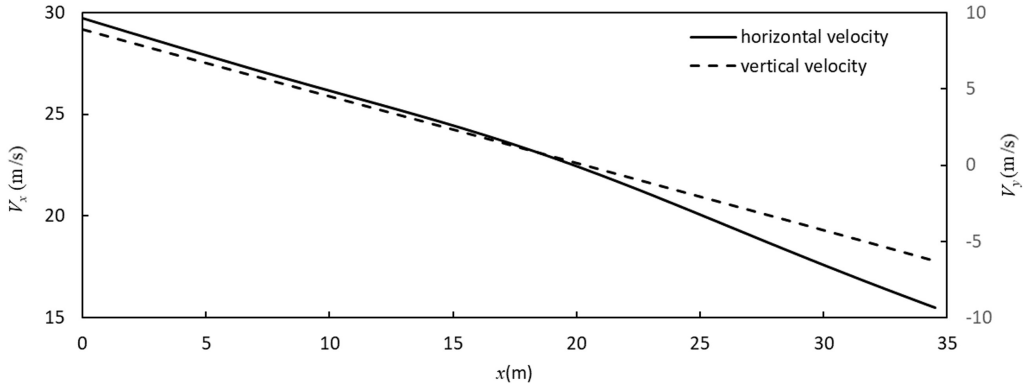


Fig. 6. Changes in horizontal and vertical components of flight velocity of the knuckleball free-kick calculated with physical constraints.

Positive Effects of Physical Constraints

With the inclusion of physical constraints, the proposed fitting model preserves a close adherence to aerodynamic principles that govern the phenomenon. To emphasize the significance of the constraint formulated in Eq. 21, Figs. 2 and 4 show the fitting outcomes without constraints, plotted as dashed lines within the plots. Both models yield highly accurate fit to the trajectory, regardless of the presence or absence of the constraints. Moreover, the unconstrained regression model exhibits superior performance, showcasing a higher coefficient of determination, $R^2 = 0.9986$. However, the unconstrained model fails to correctly depict the variation in motion speed. The dashed line in Fig. 4 illustrates that the speed undergoes multiple oscillations, rather than a monotonous decrease along the trajectory. This pattern does not comply with the established aerodynamic principle. Moreover, the absence of the physical constraint leads to the local concave shape of fitted trajectory at the initial stage. In this region, the second-order derivative is less than zero ($f'' > 0$), leading to issues with the calculation in Eq. 10 and rendering the determination of meaningful motion speed to be unattainable.

Sensitivity Analysis of Model Parameters

The polynomial order n in Eq. 19 and the weighting factor λ in Eq. 22 are two important parameters in the proposed regression model. This subsection carries out a sensitivity analysis to explore the impact of these two model parameters.

The Polynomial Degree n

Polynomial regression methods can introduce notable errors if the polynomial order is excessively low, while opting for a high order might lead to overfitting concerns. To illustrate the influence of the polynomial order, the calculated motion trajectory and drag coefficient of knuckleball free-kicks are explored using different polynomial orders, specifically n=8, n=9 and n=10. The results are visualized in Figs. 7 and 8, as well as summarized in Table 1. Fig. 7

provides a visual comparison of the three motion trajectories obtained using different orders, revealing nearly indistinguishable differences. For clarity of comparison, the trajectory for n = 8 has been shifted by 0.1 m downwards, while the trajectory for n = 10 has been shifted by 0.1 m upwards. Table 1 offers an overview of the coefficients of determination associated with the three orders. The regressions corresponding to n = 9 and n = 10 both yield a coefficient of determination of R^2 = 0.9962, while the regression with n = 8 results in a slightly lower coefficient of determination of R^2 = 0.9960. This observation suggests that n should take the value of 9, as it gives small error and avoids overfitting. Notably, it should be mentioned that the computed soccer ball speeds from the three trajectories display small disparities, although they are not herein presented.

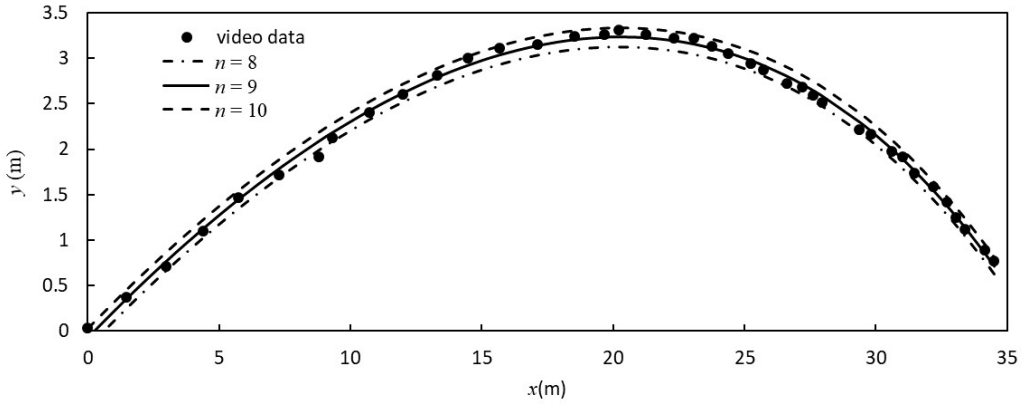


Fig. 7. Fitted trajectories of the knuckleball free-kick by using different polynomial orders.

Table 1. Coefficients of determination of fitted trajectory by using different polynomial orders.

order	n = 8	n=9	n=10
coefficient of determination R^2	0.9960	0.9962	0.9962

Fig. 8 presents the changes in drag coefficients using different polynomial orders. Evidently, the drag coefficients obtained from computations with n = 9 and n = 10 are nearly identical, while those obtained with n = 8 exhibit only a slight difference. Upon scrutinizing the three curves on the graph, it can be deduced that for $n \geqslant 9$ the fitting results of the trajectory are primarily governed by the constraint defined in Eq. 21. This observation

suggests that an increase in polynomial order does not actually give rise to overfitting complications. Further corroborating this deduction, the coefficients of determination for the cases of n = 9 and n = 10 in Table 1 underscore a consistent R^2 value of 0.9962. This consistency lends support to the conclusion that selecting a polynomial order of n = 9 engenders stable and convergent results within the scope of this study.

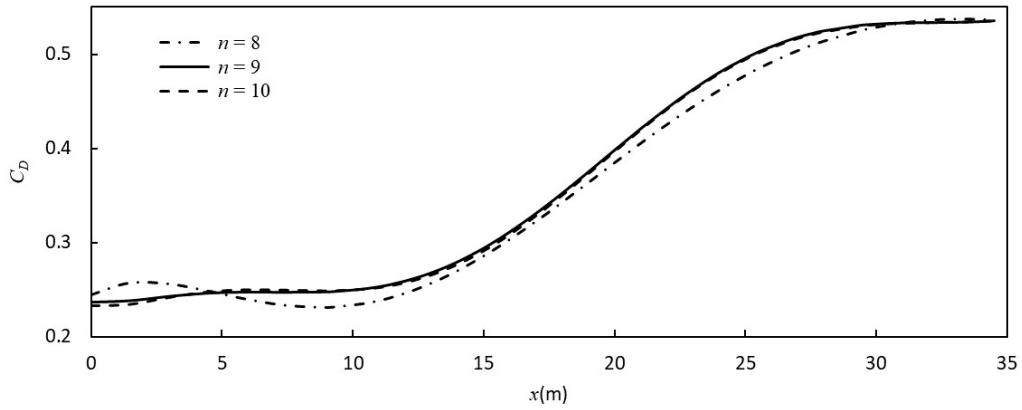


Fig. 8. Changes in drag coefficients by using different polynomial orders.

The Weighting Factor λ

Eq. 22 consists of two components. One reflects how effectively the proposed model captures the image data, while the other accounts for the discrepancy in the constraint stipulated by Eq. 21. The fine-tuning of these components is accomplished through the value of the weighting factor λ. Given the context of this study, where an accurate portrayal of free-kick trajectories forms the cornerstone of understanding the knuckleball motion characteristics, it is essential to examine its influences. Therefore, the weighting factor is chosen to be λ = 0.1, signifying that the constraint error is more tolerated than the error arising from trajectory fitting. Supplementary calculations are undertaken with λ = 0.05 and λ = 0.2, allowing for comprehensive comparisons among these three scenarios.

Much like the analysis in the preceding subsection, changing the weighting factor λ has a minor effect on both the free-kick trajectory and speed. Hence, elaborate comparisons are omitted in this subsection. Fig. 9 shows the changes in drag coefficients resulting from

altering the weighting factor. The graph shows that the drag coefficients calculated using λ = 0.1 and λ = 0.05 are remarkably consistent, while the result computed with λ = 0.2 displays a marginal discrepancy, primarily in the middle stage of the flight. This discrepancy indicates that, when λ = 0.2, the constraint outlined by Eq. 21 is overemphasized in the fitting process. However, within the range of 0.05 < λ < 0.1, the fitting results display limited sensitivity to the weighting factor. Therefore, in the context of this study, the fitting results are reasonable and trustworthy with the selection of λ = 0.1.

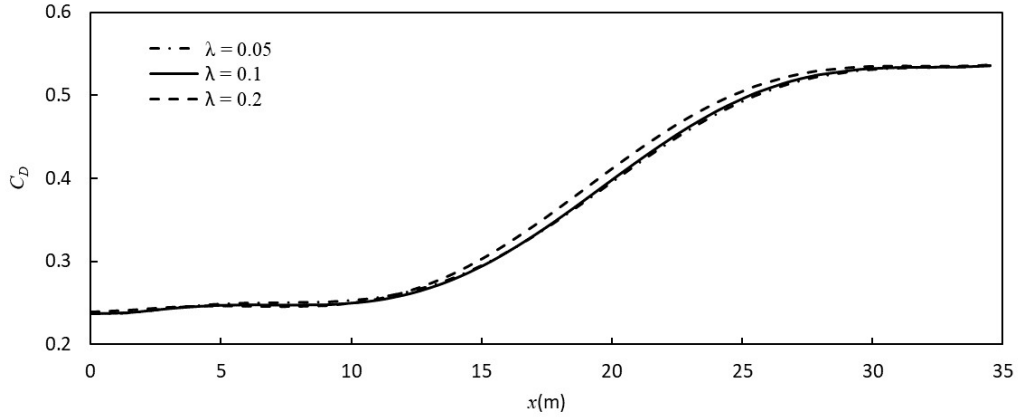


Fig. 9. Changes in drag coefficients by using different weighing factors.

Conclusions

This study aims to capture the knuckleball free-kick's distinct trajectory and the accompanied aerodynamic characteristics, which have captivated soccer enthusiasts and researchers alike. This study introduces an innovative approach to analyze the knuckleball free-kick trajectory executed by Cristiano Ronaldo in a match between Real Madrid and Atletico Madrid in April 2012. The discrete points of the trajectory are obtained by employing image processing techniques. By establishing a physical constraint based on the relationship between the free-kick trajectory, velocity, and drag coefficient, this study respects the aerodynamic principles in analyzing the knuckleball free-kick motion. The constrained polynomial regression model is implemented using MATLAB. This model offers a comprehensive analysis of the motion of knuckleball free-kicks. The model gives quantitative predictions of the displacement and

velocity of Cristiano Ronaldo's free-kick. By delving into the influences of the constraint and model parameters, the credibility of the analysis is bolstered.

The proposed constrained polynomial regression model exhibits computational efficiency, simplicity and effectiveness. It offers soccer teams, enthusiasts and researchers a reliable and quantitative tool for real-time examining the intricate nature of knuckleball free-kicks. The model parameters can be tailored to certain players. Once calibrated, our numerical model can be used by coaches, strikers and goalkeepers to appreciate the influences of the air properties, ball's initial velocity and other parameters on the ball's flight path, thus assisting players to adapt to the on-site conditions in executing and defending knuckleballs. Furthermore, our efficient model can be used in computer games to create authentic ball/player interaction. The study does not consider the ball deformation and vibration, whose significance will be the topic of further investigations.

Declaration of Conflicting Interests

The authors declare that they have no known competing financial interests or personal relationships that could have appeared to influence the work reported in this paper.

Funding

We are grateful to the financial support by EPSRC (EP/N021614/1) and Cambridge Tsinghua Joint Research Initiative Fund.

Notation

The following symbols are used in this paper:

a = parameter related to drag coefficient in Eq. 3 (-);

a_n = normal component of soccer ball acceleration (m s^{-2});

a_x = horizontal component of soccer ball acceleration (m s^{-2});

A = frontal area of soccer ball (m);

b = parameter related to drag coefficient in Eq. 3 (-);

447 c_1= parameter in Eq. 16 (m^{-1});

448 C_D = drag coefficient (-);

449 d = the soccer ball's diameter (m);

450 d_1= parameter in Eq. 16 (m^{-3});

451 D = drag force (N);

452 g = gravitational acceleration (m s^{-2});

453 f = function of motion trajectory (-);

454 G = gravity on soccer ball (N);

455 L = freekick distance (m);

456 m = number of discrete points (-);

457 M = soccer ball mass (kg);

458 n = polynomial degree (-);

459 R = curvature radius of motion trajectory (m);

460 R^2 = coefficient of determination (-);

461 Re = Reynolds number (-);

462 V = soccer ball speed during the flight (m s^{-1});

463 V_c = critical speed (m s-1);

464 V_s = parameter related to drag coefficient in Eq. 3 (m s^{-1});

465 x = horizontal position of soccer ball (m);

466 y = vertical position of soccer ball (m);

467 $\alpha = [\alpha_0, \alpha_1, \cdots, \alpha_n]^T$ = polynomial parameter (-);

468 λ = weighting factor (-);

469 ρ = air density (kg m^{-3});

470 θ = angle between flying direction and horizontal plane (rad);

References

1. Asai T, Kimachi K, Liu R, et al. Measurements of the flight trajectory of a spinning soccer ball and the Magnus force acting on it. *Proceedings* 2020; 49: 88.
2. Eager D, Ishac K, Zhou S and Hossain I. Investigating the Knuckleball Effect in Soccer Using a Smart Ball and Training Machine. *Sensors* 2022; 22: 3984.
3. Borg J and Morrissey M. Aerodynamics of the knuckleball pitch: experimental measurements on slowly rotating baseballs. *Am J Phys* 2014; 82: 921-927.
4. Cobb T, Cobb WR and Dickson P. *My twenty years in baseball*. Mineola, NY: Dover, 2009.
5. Hoffman J and Johnson J. Secrets of Ball Sports. In: Hoffman J and Johnson C (eds) *Computational Turbulent Incompressible Flow*. Berlin, Heidelberg: Springer, 2007, pp. 175–180.
6. Hong S, Chung C, Sakamoto K, et al. Analysis of the swing motion on knuckling shot in soccer. *Procedia Eng* 2011; 13: 176-181.
7. Mehta R. Aerodynamics of sports balls. *Annu Rev Fluid Mech* 1985; 17: 151–189.
8. Goff JE and Carre MJ. Soccer ball lift coefficients via trajectory analysis. *Euro J Phys* 2010; 31: 775-784.
9. Passmore M, Rogers D, Tuplin S, et al. The aerodynamic performance of a range of FIFA-approved footballs. *Proc Inst Mech Eng P J Sports Eng Technol* 2012; 226(1): 61-70.
10. Barber S, Haake SJ and Carré MJ. Using CFD to understand the effects of seam geometry on soccer ball aerodynamics. In: Moritz EF, Haake S (eds) *The Engineering of Sport 6*, Vol. 2. New York: Springer, 2006, pp. 127–132.
11. Jourdan G, Houas L, Egra O, et al. Drag coefficient of a sphere in a non-stationary flow: new results. *Proc R Soc* 2007; 463(2088): 3323-3345.
12. Goff JE. Power and spin in the beautiful game. *Phys Today* 2011; 63: 62–63.
13. Mizota T, Kurogi K, Ohya Y, et al. The strange flight behavior of slowly spinning soccer balls. *Sci Rep* 2013; 3: 1871.

14. Asai T and Kamemoto K. Flow structure of knuckling effect in footballs. *J. Fluids Struct* 2011; 27: 727-733.

15. Texier BD, Cohen C, Quere D. Physics of knuckleballs. *New J Phys* 2016; 18: 073027.

16. Barber S, Chin SB and Carre MJ. Sport ball aerodynamics: A numerical study of the erratic motion of soccer balls. *Comput Fluids* 2009; 38: 1091-1100.

17. Pellow R. Cristiano Ronaldo: When Man Utd star took part in awful free-kick routine at Juventus. https://www.givemesport.com/87970020-cristiano-ronaldo-when-man-utd-star-took-part-in-awful-free-kick-routine-at-juventus/ (2020, accessed 28 July 2023).

18. The Weather Company. Weather underground. https://www.wunderground.com/history/daily/es/madrid/LEMD/date/2012-4-11 (2012, accessed 28 July 2023).

19. García-Herrero J, Sanchez-Sanchez J, Luis-Pereira J, et al. The effects of induced variability in the performance on shot in soccer. *Intern J Sports Sci Coach* 2016; 11(5): 648–654.

20. Kray T, Franke J. and Frank W. Magnus effect on a rotating soccer ball at high Reynolds numbers. *Journal of Wind Engineering & Industrial Aerodynamics* 2014;124: 46-53

21. Goff JE, Smith WH and Carre MJ. Football boundary-layer separation via dust experiments. *Sports Eng* 2011; 14:139-146.

22. Tada K, Hiratsuka M, Ito S, et al. Effect of surface design on drag properties of soccer balls. *The Japan Society of Mechanical Engineers* 2023, 89(924): 23-00045.

23. Alam F, Chowdhury H, Stemmer M, et al. Effects of surface structure on soccer ball aerodynamics. *Procedia Eng* 2012; 34: 146-151.

24. Alam F, Chowdhury H, George S, et al. Aerodynamic drag measurements of FIFA-approved footballs, *Procedia Eng* 2014; 72: 703-708.

25. Asai T and Hong S. Aerodynamics of the newly approved football for the English Premier League 2020–21 season. *Sci Rep* 2021; 11:9578.

26. Scott J and Tuma M. Solving large linear least squares problems with linear equality constraints. *Bit Numer Math* 2022; 62:1765–1787.

27. The MathWorks Inc. MATLAB version: 9.13.0 (R2022b), Natick, Massachusetts: The MathWorks Inc. https://www.mathworks.com (2022, accessed 28 July 2023).
28. Dougherty ER, Kim S and Chen Y. Coefficient of determination in nonlinear signal processing. *Signal Processing* 2000; 80(10): 2219-2235.
29. Dermot C. The six best goals of Cristiano Ronaldo's La Liga career. https://www.espn.co.uk/football/story/_/id/37492375/the-six-best-goals-cristiano-ronaldo-la-liga-career (2018, accessed 28 July 2023).
30. Asai T, Seo K, Kobayashi O, et al. Fundamental aerodynamics of the soccer ball. *Sports Eng* 2007; 10(2): 101–109.

Appendix – Raw Dataset

Table A1. Original data and fitted results for the case n=9 with the polynomial parameter α= [-0.0724, 10.4640, -7.0799, -1.6177, -0.8602, 3.9957, -10.1578, 8.9066, -3.5557, 0.4920]^T, in which f, y, x are all measured in meters.

Original data		Fitted results				
x	y	f	f'	f''	f'''	f''''
0	0.037252	-0.072400	3.488E-01	-1.573E-02	-3.595E-04	-2.549E-05
1.464031	0.372987	0.352795	3.288E-01	-1.620E-02	-3.790E-04	-7.972E-06
2.990241	0.707786	0.768879	3.072E-01	-1.670E-02	-3.847E-04	-2.491E-06
4.380081	1.099089	1.122945	2.871E-01	-1.716E-02	-3.889E-04	-5.761E-06
5.738678	1.471923	1.445518	2.668E-01	-1.762E-02	-4.001E-04	-1.420E-05
7.291124	1.713993	1.784829	2.430E-01	-1.817E-02	-4.277E-04	-2.776E-05
8.807955	1.918472	2.085287	2.190E-01	-1.875E-02	-4.736E-04	-4.295E-05
9.295951	2.123440	2.175260	2.112E-01	-1.895E-02	-4.926E-04	-4.795E-05
10.71207	2.402747	2.417447	1.878E-01	-1.959E-02	-5.595E-04	-6.218E-05
11.99179	2.607699	2.611499	1.659E-01	-2.024E-02	-6.343E-04	-7.410E-05
13.29315	2.812518	2.783842	1.429E-01	-2.100E-02	-7.231E-04	-8.479E-05
14.46281	2.998778	2.916469	1.215E-01	-2.177E-02	-8.123E-04	-9.293E-05
15.68509	3.110534	3.031661	9.824E-02	-2.267E-02	-9.135E-04	-9.983E-05
17.13265	3.147785	3.135800	6.937E-02	-2.388E-02	-1.041E-03	-1.059E-04
18.5176	3.240914	3.201026	4.026E-02	-2.519E-02	-1.170E-03	-1.098E-04
19.65628	3.259541	3.228132	1.509E-02	-2.639E-02	-1.278E-03	-1.119E-04
20.22359	3.315473	3.232326	2.107E-03	-2.702E-02	-1.332E-03	-1.126E-04
21.23592	3.259594	3.223834	-2.186E-02	-2.822E-02	-1.431E-03	-1.136E-04
22.3268	3.222344	3.190862	-4.889E-02	-2.961E-02	-1.537E-03	-1.145E-04
23.08321	3.222343	3.152873	-6.841E-02	-3.063E-02	-1.612E-03	-1.152E-04
23.765	3.129215	3.107610	-8.659E-02	-3.159E-02	-1.679E-03	-1.160E-04
24.363	3.054712	3.059039	-1.030E-01	-3.247E-02	-1.739E-03	-1.169E-04
25.22914	2.942900	2.973497	-1.276E-01	-3.379E-02	-1.826E-03	-1.187E-04
25.72225	2.868457	2.916525	-1.420E-01	-3.457E-02	-1.877E-03	-1.201E-04
26.61922	2.719454	2.796953	-1.692E-01	-3.605E-02	-1.970E-03	-1.234E-04
27.19092	2.682137	2.709677	-1.871E-01	-3.703E-02	-2.031E-03	-1.261E-04
27.62213	2.589075	2.637977	-2.009E-01	-3.779E-02	-2.078E-03	-1.286E-04
27.94416	2.514779	2.581068	-2.114E-01	-3.837E-02	-2.114E-03	-1.306E-04
29.36554	2.216488	2.294345	-2.598E-01	-4.105E-02	-2.280E-03	-1.424E-04
29.82331	2.160932	2.189225	-2.761E-01	-4.195E-02	-2.337E-03	-1.473E-04

30.61029	1.974702	1.993329	-3.049E-01	-4.356E-02	-2.439E-03	-1.569E-04
31.01233	1.918472	1.885650	-3.201E-01	-4.441E-02	-2.494E-03	-1.626E-04
31.46926	1.732214	1.756861	-3.377E-01	-4.540E-02	-2.559E-03	-1.696E-04
32.19577	1.583204	1.537684	-3.664E-01	-4.703E-02	-2.669E-03	-1.823E-04
32.68888	1.415695	1.378569	-3.866E-01	-4.817E-02	-2.748E-03	-1.919E-04
33.03649	1.248078	1.261243	-4.010E-01	-4.900E-02	-2.806E-03	-1.992E-04
33.39327	1.117556	1.136298	-4.162E-01	-4.987E-02	-2.868E-03	-2.072E-04
34.1539	0.894047	0.854245	-4.493E-01	-5.179E-02	-3.009E-03	-2.260E-04
34.50565	0.765709	0.716418	-4.650E-01	-5.270E-02	-3.079E-03	-2.354E-04

539